PROGRESS ON TISSUE-LEVEL, FUNCTIONAL TOLERANCE CRITERIA AND MATERIAL PROPERTIES OF THE LIVING BRAIN WITH ANATOMICAL RESOLUTION

Barclay Morrison III, Zhe Yu, Benjamin S. Elkin
Department of Biomedical Engineering, Columbia University, New York, USA

ABSTRACT

Determining failure limits for biological tissues is necessary for predicting the injury potential of a loading scenario. For brain tissue, cell death and changes in electrophysiological function are more meaningful than mechanical failure criteria. Interim data is presented on a functional tolerance criterion for the hippocampus. In addition, material properties of the hippocampus were measured with the atomic force microscope. The CA1 subfield was significantly stiffer than the rest of the hippocampus. Both the tolerance criterion and material properties can be incorporated into computer models to increase their biofidelity and extend their capabilities to predict biological outcomes.

Keywords: Biomechanics, Brain, Injury Criteria, Soft Tissues

IN 2006, the International Research Council on the Biomechanics of Impact (IRCOBI) released a review titled "Future research directions in injury biomechanics and passive safety research" which summarized research areas believed to have the greatest potential to reduce injuries. One of the central questions posed was "How can we better characterize the mechanisms by which these [human structures, subsystems, and] components undergo mechanical failure?" Failure is a central theme of our studies on brain tissue, and our studies have benefited from a broader definition of failure, particularly for brain.

Mechanical failure may be an adequate definition of failure for some components of the human body, particularly load-bearing tissues like bone. Even for soft tissues, in the most severe sense, injury can be defined as mechanical failure evidenced by macroscopic disruption of mechanical continuity resulting in tearing or frank hemorrhage, for example. However, tearing of tissue or cells within tissue is only one mode of failure, and many other modes of failure may exist for biological tissues.

A fundamental difference between inert engineering materials and biological tissues is that the latter is alive and performs some form of active function. Therefore, the very concept of failure must be revised for living tissues. The exact definition may be tissue-specific such as fracture for bone or laceration for skin. However, these definitions may be too insensitive to identify the onset of injury or tolerance criteria for the brain. For non-load-bearing, living, cellular tissues, failure can be defined in a myriad of ways which may occur at levels of mechanical stimulus far below mechanical failure. For example, it may not be necessary to rip apart a cell to kill it, or tear a neuron to affect its function.

For brain and other highly cellular tissues cell death may be a widely applicable outcome. We have previously applied this definition and determined tissue-level tolerance criteria for cell death in the rat hippocampus and cortex (Cater et al., 2006; Elkin and Morrison III, 2007). In these studies, cultured slices of brain tissue were subjected to controlled mechanical deformation, and the resultant cell death quantified in a region-specific manner (Morrison III et al., 2006). We developed empirical relationships between input mechanical stimuli (tissue strain) and cell death. The goal was to provide these functions for incorporation into finite element (FE) models, providing them with the capability to predict biological responses in addition to typical mechanical parameters such as stress and strain.

Herein, we propose an additional measure which is more specific to nervous system tissue, disruption of electrophysiological function. In the present study, we have begun to quantify changes in evoked field potentials four days after injury. As we quantify the post-traumatic electrophysiological function for more combinations of injury parameters (strain and strain rate), we will develop region-specific tolerance criteria for neuronal function to complement our earlier cell death criteria. However, an operational definition of failure still remains to be determined that captures the change in electrophysiological function which constitutes a biologically relevant dysfunction or failure.

We study the response of living brain tissue to mechanical stimuli below ultimate failure. In our previous studies, cell death was not induced instantaneously during the mechanical stimulus, but required days to develop (Cater et al., 2006; Elkin and Morrison III, 2007). These findings highlight a distinction between engineering materials and biological tissues, which the 2006 IRCOBI review begins to highlight at a macroscopic, whole body level when it notes that "humans are not inanimate systems but rather ones which can react, via muscle response". Although only muscle response is mentioned, this responsiveness applies to all levels of scale including cellular and molecular.

Biological tissues, and the cells within those tissues, constantly respond to environmental stimuli, including mechanical stimuli. These responses include signaling cascade activation, gene expression changes, cytoskeleton remodeling, cell movement, etc. Depending on the magnitude of the stimulus, the reaction may be a normal physiological response or, as in the case of impact injury, a pathological response resulting in disruption of tissue function or cell death. Although the mechanical stimulus may be severe enough to cause mechanical failure of the tissue, lower stimuli can induce damage and dysfunction in a delayed fashion as the processes of mechano-transduction unfold over time.

FE models provide the critical link between macroscopic loading parameters and the resultant mechanical reaction at the tissue level. The input mechanical stimulus is ultimately responsible for the biological outcome. Through computational models, laboratory experiments at the tissue level can be translated to predict tissue-level responses to real-world injury scenarios. FE models are becoming increasingly important in automotive and safety system design and perhaps in the legislative domain in the future (Takhounts et al., 2003b; Takhounts et al., 2008).

For computational models to accurately predict biological outcomes, they first must accurately predict the mechanical response at the tissue level, which requires appropriate material properties. Measuring material properties of the brain poses particular challenges. Brain is one of the softest tissues in the body and to measure reaction forces during testing requires either very sensitive transducers or large samples (Hrapko et al., 2006; Nicolle et al., 2004; Coats and Margulies, 2005; Gefen et al., 2003; Prange and Margulies, 2002). Brain is structurally heterogeneous with gray and white matter at the grossest level of distinction with many finer features apparent upon histological examination. The use of large samples precludes measuring the properties of these finer structures.

One motivation to measure material properties of the brain's substructures or components is that others have shown that inclusion of heterogeneous material properties in computational models provides more accurate predictions of induced tissue damage (Zhang et al., 2001). Only by inclusion of particular anatomical structures within a model can the predicted injury pattern be compared and validated against histological sections of the true injury pattern. For example, the CA3 pyramidal layer of the hippocampus is particularly vulnerable to fluid percussion injury (FPI) models of TBI (Hicks et al., 1996; Smith et al., 1997; Morales et al., 2005). Predicting this preferential cell loss in CA3 with a computational model would be a substantial step toward its validation. But, only by inclusion of a hippocampus with a CA3 subfield will that be possible.

We were further motivated to measure the mechanical properties of the hippocampus by findings in our tissue culture injury model that CA1 and CA3 were equally vulnerable to strain-induced cell death (Cater et al., 2006; Morrison III et al., 2003). Our data were in contrast to experimental findings that CA3 was preferentially vulnerable to FPI *in vivo* (Hicks et al., 1996; Smith et al., 1997). One explanation was that our injury model induced deformation by the controlled stretch of the substrate to which the brain tissue cultures were adhered. The substrate is several orders of magnitude stiffer than the brain tissue, so its deformation is not appreciably affected by the cultured slice. In contrast, in the experimental animal models, a pressure pulse is applied to the surface of the brain, whereby the induced, local tissue strain depends on the regional mechanical properties of the brain. This heterogeneity may be as complex as the heterogeneous structure evident in histological sections. Therefore, we hypothesized that the CA3 region is more compliant than other hippocampal regions giving rise to larger local deformations and hence greater cell death in CA3 *in vivo*.

To test our hypothesis, we have used the atomic force microscope (AFM) to measure mechanical properties within specific anatomical structures of the brain. We have found that the adult hippocampus is mechanically heterogeneous and that compared to CA1, the CA3 region is more compliant, potentially explaining is preferential vulnerability to FPI.

METHODS

ORGANOTYPIC SLICE CULTURES: All animal procedures were approved by the Columbia University IACUC. Hippocampal slice cultures were cultured as previously described (Morrison III et al., 2006). Briefly, the hippocampus of a 10 day old rat pup was dissected, sliced into 400µm sections and plated into custom culture wells. The well's center contained a silicone membrane pre-coated with laminin and poly-lysine for adhesion. Cultures were maintained at 37ºC with 5% CO_2 for 10-14 days in Neurobasal medium (Invitrogen) until injured. After injury, cultures were returned to the incubator until the indicated time point for electrophysiological recording.

MECHANICAL INJURY: Brain slice cultures were injured by the deformation of their substrate, as described previously (Cater et al., 2006; Morrison III et al., 2003). In brief, the silicone membrane was deformed by pulling the well down over a rigid, hollow, cylindrical indenter, inducing an equi-biaxial stretch. Uninjured, control cultures were places on the injury device, but the actuator was not energized. The relative motion between the two was under feedback control so that the strain history was precisely controlled (strain and rate). A significant advantage of this model was that the culture deformation could be verified from high speed video (Redlake, 1000 fps). The maximum applied Lagrangian strain was determined by measuring the area of the slice before stretch (A_0) and at the maximal stretch (A_{max}) according to:

$$E_{\text{Lagrangian}} = \frac{1}{2}\left(A_{max}/A_o - 1\right)$$

ELECTROPHYSIOLOGICAL RECORDINGS: After injury or sham injury, cultures were transferred to 60 electrode microelectrode arrays (MEA, MultiChannel Systems, Fig. 1A). Stimuli of varying magnitudes (0µA-200µA in 10µA steps) delivered within the mossy fibers of the dentate gyrus with a programmable stimulator (MultiChannel Systems) elicited evoked electrophysiological responses which were recorded on the other 58 channels. The magnitude of the evoked response was determined as the peak to peak value after the stimulus artifact (Fig. 1B).

Responses were grouped by the anatomical location of the recording electrode (CA1, CA3, DG). The response magnitude was plotted as a function of stimulus intensity and fit to a sigmoidal function to parameterize the response (Fig. 1C) in which R(S) was the response magnitude in µV, R_{max} was the maximal response in µV, S was the stimulus intensity in µA, I_{50} was the stimulus intensity in µA which resulted in a half-maximal response, and m was a dimensionless parameter proportional to the slope of the linear region of the curve:

$$R(S) = \frac{R_{\max}}{1 + e^{m \bullet (I_{50} - S)}}$$

Data is presented as mean ± standard error of the mean. Given the subset of data, a full two-way ANOVA could not be performed. Instead, data was analyzed with a one way ANOVA to test for an injury effect followed by post-hoc tests with Bonferroni corrections to determine which groups were different from controls within a recording region. Significance was set at $\alpha \leq 0.05$.

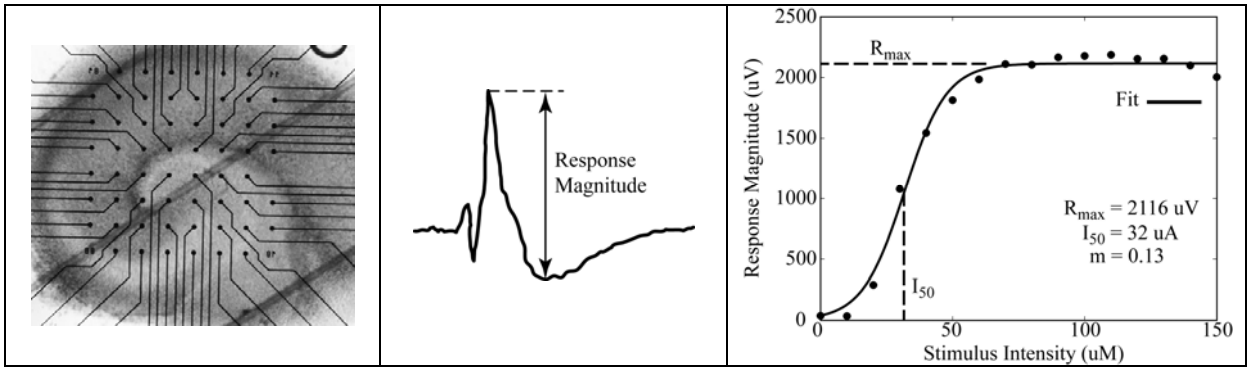

Fig. 1A. Slice Culture on MEA B. Quantification of Response C. Stimulus Response Curve with Fit

AFM INDENTATION TESTING: Coronal sections of adult rat brain were cut and plated in medium as above. All mechanical testing was performed on a heated stage to maintain the tissue at 37ºC and in culture medium. Indentations were performed with a Bioscope AFM (Veeco). Cantilever probes were modified with 12.5µm radius sphere and calibrated by the manufacturer (NovaScan, spring constant = 0.13-0.16 N/m). Indentations were performed at 1Hz in 6 x 6 arrays with a spacing of 6µm in the following anatomical locations within the hippocampus (Fig. 2): CA1 and CA3 pyramidal cell layers shown in gray (CA1P and CA3P, respectively), CA1 and CA3 stratum radiatum shown in black (CA1SR and CA3SR, respectively), and the dentate gyrus shown in gray (DG).

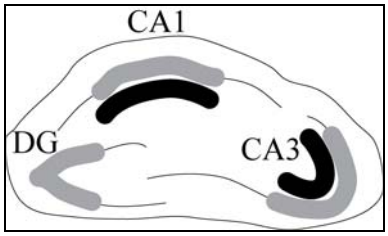

Fig. 2 Indentation Locations

A depth-dependent, pointwise elastic modulus ($\hat{E}$) was determined by the following equation with *h* the cantilever deflection, *k* the cantileverspring constant, ν Poisson's ratio, *R* the probe radius, *D* the indentation depth, and *a* the contact radius (Sneddon, 1965; Harding and Sneddon, 1945):

$$\hat{E}(D) = \frac{3\left(1-\nu^2\right)\bullet k \bullet h}{4\sqrt{RD^3}} \quad given \quad D = \frac{1}{2}a\log\frac{R+a}{R-a}$$

The contact point was identified as previously described (Elkin et al., 2007). Briefly, a high-order polynomial was fit to the raw deflection versus displacement curves. The contact point was identified as the first point with both positive first and second derivatives above an empirically determined threshold which was applied to all curves.

The pointwise elastic modulus $\hat{E}$ at 3µm indentation depth was compared between regions by a one-way ANOVA followed by post-hoc tests with Bonferroni corrections ($\alpha \leq 0.05$).

CONSTITUTIVE MODELING: The depth-dependent, non-linear, elastic properties for depths greater than 250nm were fit to the following constitutive models from (Ogden, 1972), (Gou, 1970), and (Demiray, 1972), respectively.

$$W = \frac{2\mu}{\alpha^2}(\lambda_1^\alpha + \lambda_2^\alpha + \lambda_3^\alpha - 3)$$

$$W = c\left(e^{kI_1\left(I_1^2 - 3I_2\right)} - 1\right)$$

$$W = \frac{\beta}{2\alpha}\left(e^{\alpha(I_1-3)} - 1\right)$$

The material was assumed to be incompressible and the constitutive models were exercised under uniaxial compression with strain defined as (Kalidindi and Pathak, 2008):

$$\varepsilon = \frac{4D}{3\pi a} \quad such\ \ that \quad \lambda = 1 - \frac{4D}{3\pi a}$$

The goodness of fit was determined by calculating the mean square error (MSE) normalized to the MSE of the data. Fit parameters are presented as mean ± 95% confidence intervals.

DYNAMIC AFM INDENTATION: The AFM indentation studies were extended to the viscoelastic regime following previously published methods (Mahaffy et al., 2004; Mahaffy et al., 2000). A small oscillatory indentation was superimposed on the static indentation, and a lock-in amplifier (SR830, Stanford Research Systems) measured the phase difference between the driving oscillation of the cantilever and the oscillatory deflection of the cantilever. For these preliminary results, a hydrogel of 0.25% agarose was tested; brain was not tested.

VISCOELASTIC CONSTITUTIVE MODELING: It was assumed that $\tilde{\delta}^*$, the oscillatory displacement of the cantilever probe tip, was small compared to the static displacement. Retaining only the oscillatory components of the Taylor expansion of the Hertzian solution for contact provided:

$$f^*_{osc} = 2\sqrt{R\delta_o}\,\frac{E^*}{(1-\nu^2)}\cdot\tilde{\delta}^*$$

In this case, both $\tilde{\delta}^*$ and E^* were complex variables with a frequency and phase angle. The cantilever dynamic drag force was calculated from cantilever deflection, in free medium by:

$$f^*_{drag} = i\varpi\cdot\gamma\cdot\tilde{\delta}^*$$

The frequency dependent storage (*E*') and loss (*E*") moduli were then calculated from the following equations where φ was the phase difference between the scanner displacement (drive signal) with magnitude a_d and cantilever displacement (output signal) with magnitude a_r, and k was cantilever stiffness (Mahaffy et al., 2004):

$$E_1' = \frac{(1-\nu^2)}{2\sqrt{R\delta_o}}\cdot\frac{a_d k a_r\cos\varphi - k a_r^2}{a_d^2 - 2a_d a_r\cos\varphi + a_r^2}$$

$$E_1'' = -\frac{(1-\nu^2)}{2\sqrt{R\delta_o}}\cdot\left[\frac{a_d k a_r\sin\varphi}{a_d^2 - 2a_d a_r\cos\varphi + a_r^2} + \varpi\cdot\gamma\right]$$

RESULTS

Image analysis verified the level of strain applied to each culture during the mechanical event, and each culture was assigned to the appropriate injury group. Controlled mechanical deformation induced significant changes in electrical activity at 4 days post-injury (Fig. 3). In general, R_{max} was decreased in all regions (CA1, CA3, DG) after injury, although some biological variability was present in the data. For example in all regions after an injury of 5% strain at 10/s strain rate, R_{max} remained close to control values. In the CA3 and DG region, a similar lack of effect was measured after an injury of 10% strain and 20/s strain rate.

The stimulus intensity required to evoke a half maximal response (I_{50}) decreased after the mildest injury of 5% strain at 0.1/s strain rate. This was the only group which responded with a decrease in I_{50}, indicating an increased excitability of the tissue. As the strain rate increased but strain remained constant at 5%, the I_{50} increased in both the CA1 and CA3 regions indicating a decreased excitability. After 10% strain, the effect of injury on I_{50} diminished as the strain rate increased from 5/s to 20/s

Average elastic modulus for each hippocampal region probed is presented (Fig. 4) at an indentation depth of 3µm. Statistical tests determined that CA1P was the stiffest region compared to all others. CA1SR was the second stiffest and was significantly different from any others. CA3P and CA3SR were not different from one another. The DG was the most compliant region and was significantly softer than all other regions tested.

The indentation depth dependence of $\hat{E}$ is shown in Fig. 5 for indentations greater than 250nm. The different constitutive models were fit to the data and yielded normalized MSEs of 1.13, 1.15, and 1.16 for the Ogden, Gou, and Demiray models, respectively. The best parameter fits with 95% confidence intervals for the Ogden model by region are presented in Table 1.

Oscillatory AFM indentations were performed at two frequencies, 50 and 200Hz. The 200Hz oscillatory drive signal and the cantilever deflection are shown in Fig. 6. At 200Hz, the phase difference was 43º with a calculated storage and loss modulus of E' = 9.2 kPa, E" = 8.7 kPa. As the drive frequency decreased to 50Hz, the phase difference decreased to 8.5° with a calculated storage and loss modulus of E' = 4.9 kPa and E" = 0.7 kPa, respectively.

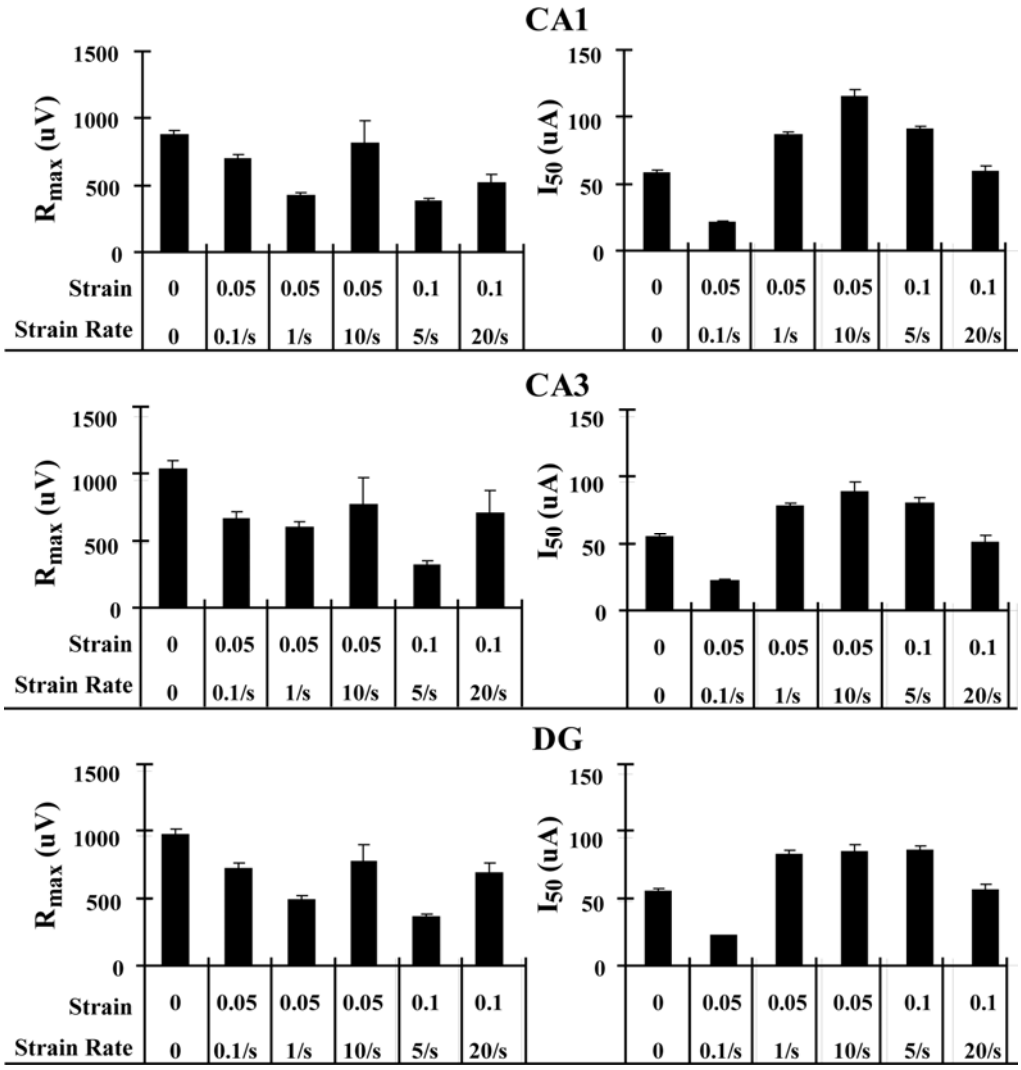

Fig. 3 Functional Response Post-Injury by Region

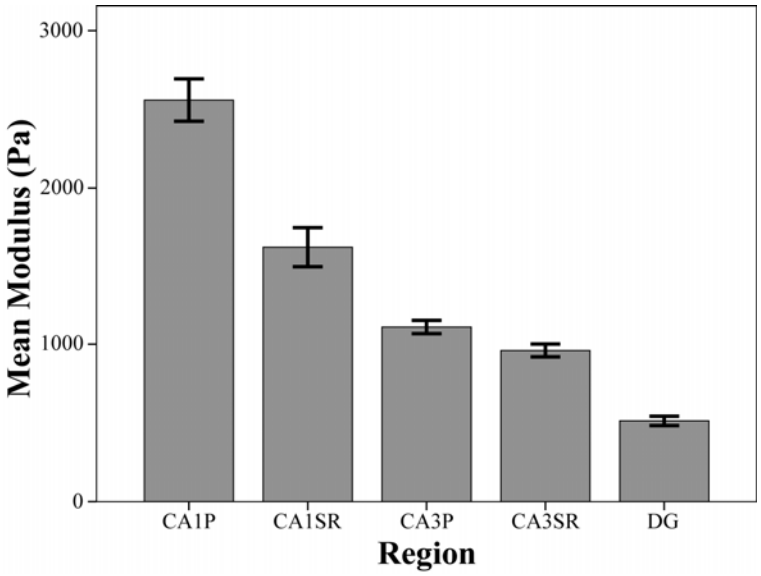

Fig. 4 Pointwise Elastic Modulus at 3µm Depth

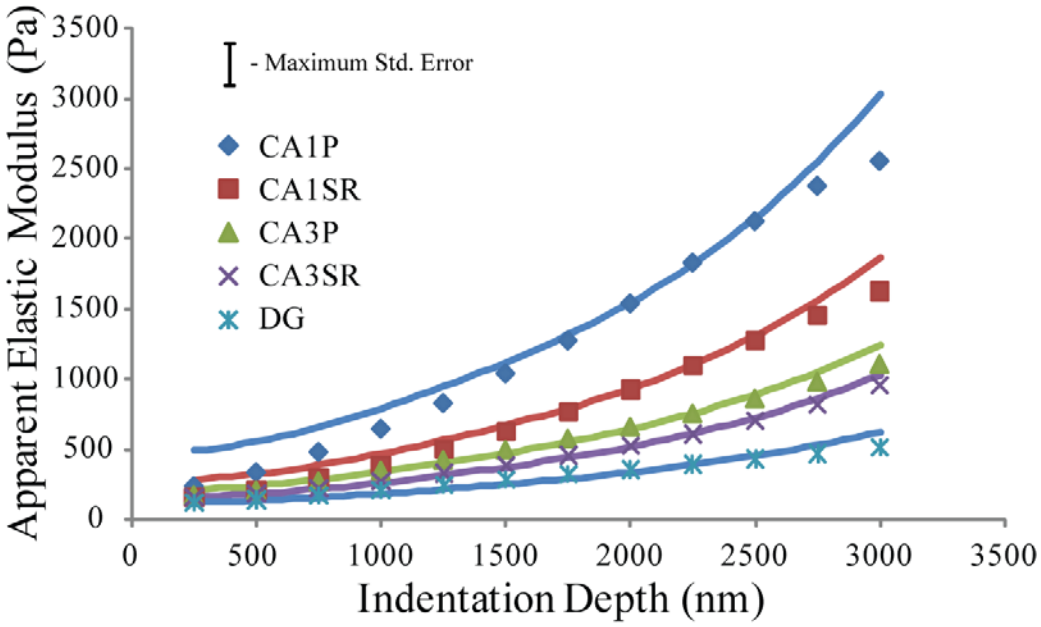

Fig. 5 Non-Linear Elastic Modulus with Constitutive Fits

Table 1. Ogden Constitutive Model Parameters

μ (Pa)		**α**	
CA1P	172.2±9.2	CA1P	31.5±0.7
CA1SR	99.6±9.0	CA1SR	32.2±1.2
CA3P	75.2±2.7	CA3P	30.8±0.5
CA3SR	55.9±2.5	CA3SR	32.0±0.6
DG	42.6±2.2	DG	29.4±0.7

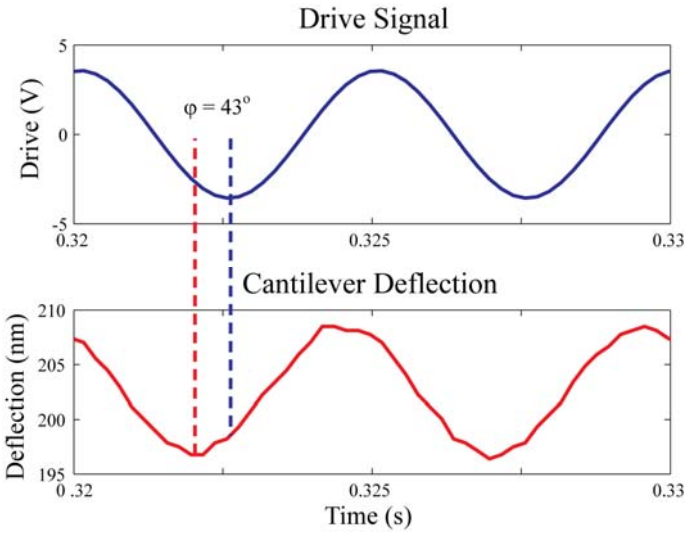

Fig. 6 Sinusoidal AFM Indentation

DISCUSSION

Finite element modeling of TBI requires certain enabling data. Our activities are providing: tolerance criteria and mechanical properties. Mechanical properties are critical for predicting accurate brain deformation in response to macroscopic, whole-body loads. Tissue-level tolerance criteria provide the capability to interpret the predicted deformation in terms of biological outcome.

We have begun to define a mechanical injury tolerance criterion for disruption of neuronal function in hippocampal slice cultures. We focused on the hippocampus because it is one of the most vulnerable regions following TBI in animal models (Hicks et al., 1996; Smith et al., 1997; Grady et al., 2003) and in clinical experience (Ariza et al., 2006; Maxwell et al., 2003), which we reproduced in our previous cell death criteria studies (Cater et al., 2006; Elkin and Morrison III, 2007). We have chosen to use an *in vitro* approach to characterize the response of living brain tissue to mechanical stimuli. Only with living tissue can changes in neuronal activity be studied. The *in vitro* approach also allows for precise control over the applied injury biomechanics (Morrison III et al., 2003; Cater et al., 2006) to determine tolerance criteria correlated with tissue-level biomechanics.

Another advantage of the *in vitro* approach is that MEA can be used to quantify function. The MEA, with 60 closely spaced electrodes, records from locations throughout the trisynapic circuitry which is maintained within the cultures (Gutierrez and Heinemann, 1999). With MEA, the neuronal circuit as a whole is interrogated as opposed to only single locations as with traditional glass electrode methods. The major disadvantage of MEAs is that they are rigid, being manufactured on glass. Consequently, the tissue cannot be cultured directly on them for injury. Instead, injuries are performed in custom culture wells with silicone bottoms. The cultures are then transferred to the MEA at the desired time point. The inclusion of uninjured sham tissue which underwent the same transfer process serves as a control for its potential non-specific effects on function.

The *in vitro* model does have other limitations which must be born in mind when interpreting results. One limitation is that the hippocampal slice cultures are generated from 10 day old rat pups and cultured for about two weeks before injury. The cultures have been shown to mature over time *in vitro*, although at a delayed rate, suggesting that they may be equivalent to older tissue but younger than a P24 animal (Collin et al., 1997; Buchs et al., 1993; Hartel and Matus, 1997; Bahr et al., 1995; Martens and Wree, 2001; Parent et al., 1997). Another limitation is the lack of a circulatory system and the potential effects, both beneficial and detrimental, of infiltrating cells on the response. These systemic factors could influence the delayed responses to injury.

In general, mechanical injury reduced the maximal evoked response from the tissue for all regions studied. This decrease suggests that either fewer neurons were firing or fewer were firing in unison. One possible mechanism is simply that the mechanical stimulus killed neurons. We would expect to induce neuronal loss with larger strains, but 5% deformation induced minimal cell loss in our previous studies (Cater et al., 2006). Therefore, an alternative explanation is that the mechanical injury affected the ability of neurons to generate action potentials, although they were still alive. Because only a subset of the full experimental matrix has been tested to date, it is difficult to speculate on potential trends in the data. There may be a strain rate dependence for the decreases in R_{max}, with 5% strain at 1/s inducing a greater deficit than 5% strain at 0.1/s, however, the results for the 5% strain 10/s group disrupt this trend. It is possible that there may be less of a rate dependence as the strain magnitude increases. After additional injury groups are generated, it will be possible to develop a predictive function relating input mechanical stimulus to functional changes.

After injury, I_{50} increased or decreased depending on the particular combination of strain and strain rate. For example, after the mildest injury of 5% and 0.1/s, I_{50} was decreased indicating that the tissue was more excitable. After other 5% strain injuries and after 10% injuries, I_{50} increased. This measure is independent of the number of functional neurons and provides insight into their excitability, whereas R_{max} is influence by both the number of neurons and their functionality. The increase of I_{50} suggests that the machinery required for neuronal function was damaged.

Only a few previous studies have quantified changes in electrical function while controlling applied strain. After optic nerve stretch injury, visually evoked potentials were significantly changed after tensile strains of approximately 25% (Bain et al., 2001). At first, this result seems at odds with ours, however, the structure of the optic nerve may be a factor. The axons within the optic nerve are arranged in a sinusoidal pattern which reduces the axonal applied strain compared to the strain of the

whole nerve. The applied axonal strains were therefore much lower than the reported 25% nerve strain (Bain et al., 2003; Bain et al., 2001). In addition, the optic nerve stretch model applies a uniaxial stretch, whereas our model employs a biaxial stretch which could be considered a more severe injury.

The majority of other studies reporting altered electrophysiology after TBI have used animal models which lack the ability to measure induced tissue deformation. Injury severity can be graded, however, changes cannot be correlated with tissue-level biomechanics. In general, evoked responses from the CA1 region were decreased after injury (Miyazaki et al., 1992; Reeves et al., 2000; Witgen et al., 2005), which agrees with the general trend of our data. Much of this decrease *in vivo* can be explained by the concomitant 40% cell loss throughout the hippocampus (Grady et al., 2003; Witgen et al., 2005). A significant finding of our current study is that the decrease in R_{max} was occurring at strains which induced minimal cell loss in our earlier studies (Cater et al., 2006).

Additional studies in the same animal models have reported increased excitability within the DG in contrast to the suppressed responses in the CA1 (Bonislawski et al., 2007; Lowenstein et al., 1992; Santhakumar et al., 2001; Santhakumar et al., 2000). We report similar findings for the most mild injury group (5% strain, 0.1/s strain rate) with a decrease in I_{50}. However, for other injury groups, excitability was suppressed as indicated by an increased I_{50}. The increased excitability *in vivo* is usually attributed to a selective loss of inhibitory neurons from within the hippocampus. Without this inhibitory input, the circuit can be stimulated to fire at lower thresholds. It is possible that the low strain injuries used in the current study did not induce this selective loss of inhibition. Instead, the injury may be disrupting the synaptic machinery within all cells, resulting in a net loss of excitability. Experiments to test specific hypotheses are required to shed further light on the causes of the changes.

We have previously reported mechanical properties of the 8 day old rat hippocampus measured with the AFM (Elkin et al., 2007). The AFM is an attractive tool for measuring brain mechanical properties for several reasons including spatial and force resolution and the ability to conduct measurements in physiological solutions at 37ºC. In the current study, we have extended our earlier results to the adult rat and find that the adult hippocampus is much stiffer overall compared to the P8 hippocampus. Different regions within the adult hippocampus have significantly different mechanical properties. The CA1 region was much stiffer than the CA3 or DG regions, suggesting that the CA3 region and DG will deform to a greater extent than the CA1 *in vivo*. In addition, our cell death tolerance indicated that the CA3 region was more susceptible to mechanical injury than the DG. Taken together, these findings predict the highest cell loss in the CA3 region of the hippocampus which is consistent with experimental findings (Hicks et al., 1996; Smith et al., 1997; Morales et al., 2005). A more quantitative prediction will require FE modeling with out data.

The mechanical response of the hippocampus was nonlinear with indentation. We have reported this nonlinearity previously for the P8 hippocampus (Elkin et al., 2007), and others have reported it for larger samples of brain (Hrapko et al., 2006; Takhounts et al., 2003a; Darvish and Crandall, 2001). We attempted to capture this response by fitting the data to nonlinear, elastic constitutive models. We found that the Ogden constitutive model fit the data best. A potential limitation of our fitting approach was that the models were assumed to undergo uniaxial strain which was approximated by the ratio of D/a. Contact radius was determined from Sneddon's closed form solution for the indentation of an elastic half-space with a spherical probe (Sneddon, 1965) which does not appear to be limited by the assumption that the indentation depth must be small compared to the radius of the indenter, as was true for earlier approximations (Harding and Sneddon, 1945). However, the strain field beneath the spherical indenter is spatially complex such that $4D/3\pi a$ is only an approximation (Kalidindi and Pathak, 2008). An inverse FE approach may be more appropriate for reproducing the AFM indentation – load curves (Husain et al., 2004).

To accurately model the dynamic brain deformations of TBI, FE models require viscoelastic properties. Our current and previous study (Elkin et al., 2007) reported modulus for slow (0.5-1Hz) indentations, which were considered to yield approximately static properties. Using a similar approach which has been applied to single cells (Mahaffy et al., 2000; Mahaffy et al., 2004), we presented a methodology to measure viscoelastic properties of brain tissue which we tested on 0.25% agarose as a surrogate for brain tissue. The viscoelastic properties were measured from sinusoidal indentations (10nm) superimposed on larger, static indentations (up to 3μm) thereby not violating assumptions inherent in the reaction force equations.

Under sinusoidal excitation, viscoelasticity is indicated by a phase difference between the driving indentation and the reaction force (Arbogast and Margulies, 1998). In our preliminary studies, the phase angle and stiffness increased with frequency. The modulus was similar to reported values (Ahearne et al., 2005; Chen et al., 2004; Gu et al., 2003). These preliminary studies indicate that it will be possible to apply this technique to brain tissue to determine frequency dependent storage and loss moduli for subregions of the hippocampus using the AFM. These properties can be incorporated into FE models which include detailed anatomical structures like the hippocampus. The FE output can then be more precisely compared to patterns of histological damage to determine its biofidelity.

CONCLUSION

Biological tissues are alive, meaning they perform active physiological functions. In the case of brain, this function ceases if the tissue is dead, which is not the case with all tissues, i.e. bone. This situation complicates TBI studies, because the tissue must be alive during the injury event to predict meaningful outcomes like cell death or changes in neuronal function. We have taken an *in vitro* approach which allows for the application of precisely controlled and verifiable mechanical stimuli to living brain tissue. We are developing mechanical tolerance criteria for disruption of neuron function within the hippocampus. In addition to the limitations noted above, a remaining challenge is to determine the degree of dysfunction at the tissue level which translates to a clinically relevant deficit.

We have used the AFM to measure mechanical properties of the brain within subregions of the hippocampus overcoming challenges of spatial and force resolution. We focused on this anatomical structure because we hypothesized that the local mechanical properties could explain its particular pattern of cell death after TBI. The CA3 region was more compliant than the CA1, predicting greater deformation and hence cell loss. The AFM methodology was successfully extended to the viscoelastic regime up to a frequency of 200 Hz. In the future, these methods will be used to determine region-specific, storage and loss moduli for incorporation into FE models. These methods are applicable to tissue from other species and other ages so as to inform pediatric-specific models, as well.

REFERENCES

Ahearne M, Yang Y, El Haj AJ, Then KY, Liu KK (2005) Characterizing the viscoelastic properties of thin hydrogel-based constructs for tissue engineering applications. J.R.Soc.Interface 2:455-463.

Arbogast KB, Margulies SS (1998) Material characterization of the brainstem from oscillatory shear tests. J.Biomechanics 31:801-807.

Ariza M, Serra-Grabulosa JM, Junque C, Ramirez B, Mataro M, Poca A, Bargallo N, Sahuquillo J (2006) Hippocampal head atrophy after traumatic brain injury. Neuropsychologia 44:1956-1961.

Bahr BA, Kessler M, Rivera S, Vanderklish PW, Hall RA, Mutneja MS, Gall C, Hoffman KB (1995) Stable maintenance of glutamate receptors and other synaptic components in long-term hippocampal slices. Hippocampus 5:425-439.

Bain AC, Raghupathi R, Meaney DF (2001) Dynamic stretch correlates to both morphological abnormalities and electrophysiological impairment in a model of traumatic axonal injury. J.Neurotrauma 18:499-511.

Bain AC, Shreiber DI, Meaney DF (2003) Modeling of microstructural kinematics during simple elongation of central nervous system tissue. J.Biomech.Eng. 125:798-804.

Bonislawski DP, Schwarzbach EP, Cohen AS (2007) Brain injury impairs dentate gyrus inhibitory efficacy. Neurobiol.Dis. 25:163-169.

Buchs PA, Stoppini L, Muller D (1993) Structural modifications associated with synaptic development in area CA1 of rat hippocampal organotypic cultures. Brain Res.Dev.Brain Res. 71:81-91.

Cater HL, Sundstrom LE, Morrison III B (2006) Temporal development of hippocampal cell death is dependent on tissue strain but not strain rate. J.Biomechanics 39:2810-2818.

Chen Q, Suki B, An KN (2004) Dynamic mechanical properties of agarose gels modeled by a fractional derivative model. J.Biomech.Eng 126:666-671.

Coats B, Margulies SS (2005) Material properties of porcine parietal cortex. J Biomech

Collin C, Miyaguchi K, Segal M (1997) Dendritic spine density and LTP induction in cultured hippocampal slices. J.Neurophysiol. 77:1614-1623.

Darvish KK, Crandall JR (2001) Nonlinear viscoelastic effects in oscillatory shear deformation of brain tissue. Med.Eng Phys. 23:633-645.

Demiray H (1972) A note on the elasticity of soft biological tissues. J.Biomechanics 5:309-311.

Elkin BS, Azeloglu EU, Costa KD, Morrison III B (2007) Mechanical heterogeneity of the rat hippocampus measured by AFM indentation. J.Neurotrauma 24:812-822.

Elkin BS, Morrison III B (2007) Region-specific tolerance criteria for the living brain. Stapp Car Crash J. 51:127-138.

Gefen A, Gefen N, Zhu Q, Raghupathi R, Margulies SS (2003) Age-dependent changes in material properties of the brain and braincase of the rat. J.Neurotrauma 20:1163-1177.

Gou P-F (1970) Strain energy function for biological tissues. J.Biomechanics 3:547-550.

Grady MS, Charleston JS, Maris D, Witgen BM, Lifshitz J (2003) Neuronal and glial cell number in the hippocampus after experimental traumatic brain injury: analysis by stereological estimation. J.Neurotrauma 20:929-941.

Gu WY, Yao H, Huang CY, Cheung HS (2003) New insight into deformation-dependent hydraulic permeability of gels and cartilage, and dynamic behavior of agarose gels in confined compression. J.Biomechanics 36:593-598.

Gutierrez R, Heinemann U (1999) Synaptic reorganization in explanted cultures of rat hippocampus. Brain Res. 815:304-316.

Harding JW, Sneddon IN (1945) The Elastic Stresses Produced by the Indentation of the Plane Surface of A Semi-Infinite Elastic Solid by A Rigid Punch. Proc.Cambridge Phil.Soc. 41:16-26.

Hartel R, Matus A (1997) Cytoskeletal maturation in cultured hippocampal slices. Neurosci. 78:1-5.

Hicks R, Soares H, Smith D, McIntosh T (1996) Temporal and spatial characterization of neuronal injury following lateral fluid-percussion brain injury in the rat. Acta Neuropathol 91:236-246.

Hrapko M, van Dommelen JA, Peters GW, Wismans JS (2006) The mechanical behaviour of brain tissue: large strain response and constitutive modelling. Biorheology 43:623-636.

Husain A, Sehgal DK, Pandey RK (2004) An inverse finite element procedure for the determination of constitutive tensile behavior of materials using miniature specimen. Comp.Mat.Sci. 31:84-92.

Kalidindi SR, Pathak S (2008) Determination of the effective zero-point and the extraction of spherical nanoindentation stress-strain curves. Acta Materialia 56:3523-3532.

Lowenstein DH, Thomas MJ, Smith DH, McIntosh TK (1992) Selective vulnerability of dentate hilar neurons following traumatic brain injury: a potential mechanistic link between head trauma and disorders of the hippocampus. J.Neurosci. 12:4846-4853.

Mahaffy RE, Park S, Gerde E, Kas J, Shih CK (2004) Quantitative analysis of the viscoelastic properties of thin regions of fibroblasts using atomic force microscopy. Biophys.J. 86:1777-1793.

Mahaffy RE, Shih CK, MacKintosh FC, Kas J (2000) Scanning probe-based frequency-dependent microrheology of polymer gels and biological cells. Phys.Rev.Lett. 85:880-883.

Martens U, Wree A (2001) Distribution of [3H]MK-801, [3H]AMPA and [3H]Kainate binding sites in rat hippocampal long-term slice cultures isolated from external afferents. Anat.Embryol.(Berl) 203:491-500.

Maxwell WL, Dhillon K, Harper L, Espin J, McIntosh TK, Smith DH, Graham DI (2003) There is differential loss of pyramidal cells from the human hippocampus with survival after blunt head injury. J.Neuropathol.Exp.Neurol. 62:272-279.

Miyazaki S, Katayama Y, Lyeth BG, Jenkins LW, DeWitt DS, Goldberg SJ, Newton PG, Hayes RL (1992) Enduring supression of hippocampal long term potentiation following traumatic brain injury in rat. Brain Res. 585:335-339.

Morales DM, Marklund N, LeBold D, Thompson HJ, Pitkanen A, Maxwell WL, Longhi L, Laurer H, Maegele M, Neugebauer E, Graham DI, Stocchetti N, McIntosh TK (2005) Experimental models of traumatic brain injury: do we really need to build a better mousetrap? Neurosci. 136:971-989.

Morrison III B, Cater HL, Benham CD, Sundstrom LE (2006) An in vitro model of traumatic brain injury utilizing two-dimensional stretch of organotypic hippocampal slice cultures. J.Neurosci.Meth. 150:192-201.

Morrison III B, Cater HL, Wang CB, Thomas FC, Hung CT, Ateshian GA, Sundstrom LE (2003) A tissue level tolerance criteria for living brain developed with an in vitro model of traumatic mechanical loading. Stapp Car Crash J. 47:93-105.

Nicolle S, Lounis M, Willinger R (2004) Shear properties of brain tissue over a frequency range relevant for automotive impact situations: new experimental results. Stapp Car Crash J. 48:239-258.

Ogden RW (1972) Large Deformation Isotropic Elasticity - Correlation of Theory and Experiment for Incompressible Rubberlike Solids. Proc.Roy.Soc.Lond.A 326:565-584.

Parent JM, Yu TW, Leibowitz RT, Geschwind DH, Sloviter RS, Lowenstein DH (1997) Dentate granule cell neurogenesis is increased by seizures and contributes to aberrant network reorganization in the adult rat hippocampus. J Neurosci 17:3727-3738.

Prange MT, Margulies SS (2002) Regional, directional, and age-dependent properties of the brain undergoing large deformation. J.Biomech.Eng. 124:244-252.

Reeves TM, Kao CQ, Phillips LL, Bullock MR, Povlishock JT (2000) Presynaptic excitability changes following traumatic brain injury in the rat. J.Neurosci.Res. 60:370-379.

Santhakumar V, Bender R, Frotscher M, Ross ST, Hollrigel GS, Toth Z, Soltesz I (2000) Granule cell hyperexcitability in the early post-traumatic rat dentate gyrus: the 'irritable mossy cell' hypothesis. J Physiol 524 Pt 1:117-134.

Santhakumar V, Ratzliff AD, Jeng J, Toth Z, Soltesz I (2001) Long-term hyperexcitability in the hippocampus after experimental head trauma. Ann.Neurol. 50:708-717.

Smith DH, Chen XH, Xu BN, McIntosh TK, Gennarelli TA, Meaney DF (1997) Characterization of diffuse axonal pathology and selective hippocampal damage following inertial brain trauma in the pig. J.Neuropathol.Exp.Neurol. 56:822-834.

Sneddon IN (1965) The relation between load and penetration in the axisymmetric Boussinesq problem for a punch of arbitrary profile. Int.J.Eng.Sci. 3:47-57.

Takhounts E, Crandall JR, Darvish KK (2003a) On the importance of nonlinearity of brain tissue under large deformations. Stapp Car Crash J. 47:79-92.

Takhounts EG, Eppinger RH, Campbell JQ, Tannous RE, Power ED, Shook LS (2003b) On the development of the SIMon finite element head model. Stapp Car Crash J. 47:107-133.

Takhounts EG, Ridella SA, Hasija V, Tannous RE, Campbell JQ, Malone D, Danelson K, Stitzel J, Rowson S, Duma S (2008) Investigation of traumatic brain injuries using the next generation of simulated injury monitor (SIMon) finite element head model. Stapp Car Crash J. 52:1-31.

Witgen BM, Lifshitz J, Smith ML, Schwarzbach E, Liang SL, Grady MS, Cohen AS (2005) Regional hippocampal alteration associated with cognitive deficit following experimental brain injury: a systems, network and cellular evaluation. Neurosci. 133:1-15.

Zhang L, Yang KH, Dwarampudi R, Omori K, Li T, Chang K, Hardy WN, Khalil TB, King AI (2001) Recent advances in brain injury research: a new human head model development and validation. Stapp Car Crash J. 45:369-393.